Quantum Chemical Calculation of Type-1 Cu Reduction Potential: Ligand Interaction and Solvation Effect

Dejun Si and Hui Li*

Department of Chemistry, University of Nebraska—Lincoln, Lincoln, Nebraska 68588

Received: June 21, 2009; Revised Manuscript Received: August 27, 2009

Using active site model molecules consisting of ~100 atoms, the reduction potentials of five type-1 Cu centers in cucumber stellacyanin, fern dryopteris crassirhizoma plastocyanin, Met148Gln rusticyanin, wild type rusticyanin, and Met148Leu rusticyanin were calculated with a heterogeneous conductor-like polarizable continuum model and the B3LYP/6-311++G(2df,p) method. The results are 242, 366, 522, 667, and 825 mV, respectively, in good agreement with experimental values 260, 376, 563, 667, and 798 mV. Ligand interaction (~250 mV) and solvation effect (~250 mV) are found to be the main determinants of the relative E^0 of these five type-1 Cu centers.

I. Introduction

Redox active proteins and enzymes containing transition metal ions are essential electron transfer components in biological systems. The reduction potential E^0 is one of the most important quantities that characterize the redox behavior of a metalloprotein. Understanding the structural factors that determine E^0 is of fundamental importance for understanding biological redox chemistry.

Quantum chemical E^0 calculation for metalloproteins remains a highly challenging task as it requires accurate descriptions of the metal−ligand interactions and protein matrix/aqueous solvation to the metal centers. Various methods have been used in the literature. For example, density functional methods have been used to calculate the E^0 of various small iron−sulfur clusters derived from proteins.[1–4] In quantum electrostatic methods,[2,5–18] the atomic charges derived from quantum chemical calculations are fixed and used in subsequent electrostatic calculations to study the protein modulations on E^0. In combined quantum mechanical and molecular mechanical methods (QM/MM), protein and solvent interactions are usually incorporated into the quantum chemical calculations of the metal centers as a reaction field and/or a force field.[1,19–24]

In principle, protein matrix should be described explicitly with structural details such as electrostatic monopoles, dipoles, and polarizabilities. Physical insights into solvation can only be obtained through MM or QM/MM simulations. Continuum models contain no specific interaction terms and can only empirically predict solvation free energies by using parametrized dielectric constants and molecular cavity sizes. Some authors have successfully parametrized and applied continuum models to describe the protein matrix and bulk aqueous solvation of protein active sites.[1,18,25,26] The author's experience in protein pK_a calculations suggests that if the active site model is relatively large (e.g., ~100 atoms), the protein matrix solvation free energy difference over a series of similar active sites can often be well reproduced by a continuum solvation model.[26] In this work, the possibility of using a continuum model to describe protein matrix and aqueous solvation in reduction potential calculation is further explored.

Due to the heterogeneous nature of the environment around an active site, the continuum solvation model should also be heterogeneous. Though the idea of using a heterogeneous continuum model has a long history, Tapia is probably the first one who developed and applied a quantum chemical heterogeneous continuum model.[27] Using heterogeneous solvation models, Tomasi's group studied the energy changes in deformations of long DNA fragments and that in the opening of a DNA double helix,[28] the partial solvation effect in molecular recognition and docking,[29] and polar solutes placed near the surface of two immiscible liquids or at a liquid/vacuum separation.[30–32] Hoshi, Sakurai, Inoue, and Chujo extended Tomasi's dielectric polarizable continuum model (DPCM) to treat anisotropic polarization effects in their guest−host complex calculations.[33] Li, Nelson, Peng, Bashford, and Noodleman developed and applied a heterogeneous continuum dielectric model to calculate the reduction potentials of 2Fe2S clusters in ferredoxin and phthalate dioxygenase reductase.[1] Recently, by using different local effective dielectrics for different portions of the solute cavity surface, Iozzi, Cossi, Improta, Rega, and Barone further extended IEF-PCM[34,35] to study the pK_a of a solvent-exposed histidine residue in prion protein and a small molecule interacting with a biological membrane.[25] Mikkelsen and co-workers developed heterogeneous solvation models for studying excited electronic states and optical properties.[36–40] In addition, the generalized Born model has been extended to treat heterogeneous environments occurring in the force field simulation of biological systems.[41–45]

In this work, a heterogeneous conductor-like polarizable continuum model (Het-CPCM) developed by the authors[46] is incorporated in the B3LYP[47–49] as a reaction field and is applied to study the E^0 of five type-1 Cu centers in cucumber stellacyanin, fern dryopteris crassirhizoma (D.c.) plastocyanin, Met148Gln, Met148Leu, and wild type *Thiobacillus ferrooxidans* (T.f.) rusticyanin, which show a 540 mV range in E^0. Large model molecules consisting of ~100 atoms are extracted from X-ray structures, and ~70 atoms are geometrically optimized. A careful examination of the calculated E^0 for 13 plastocyanins (all show E^0 ~ 370 mV) suggests that using ~100 atoms and optimizing ~70 atoms can reduce the errors caused by the structural differences in the X-ray structures to below 100 mV. Large triple-ζ basis sets with polarizable and diffuse functions are used so the Cu−ligand interactions, especially polarization, are adequately modeled. Due to the use of the Het-CPCM

* Corresponding author. E-mail: hli4@unl.edu.

10.1021/jp905825q CCC: $40.75 © 2009 American Chemical Society
Published on Web 10/07/2009

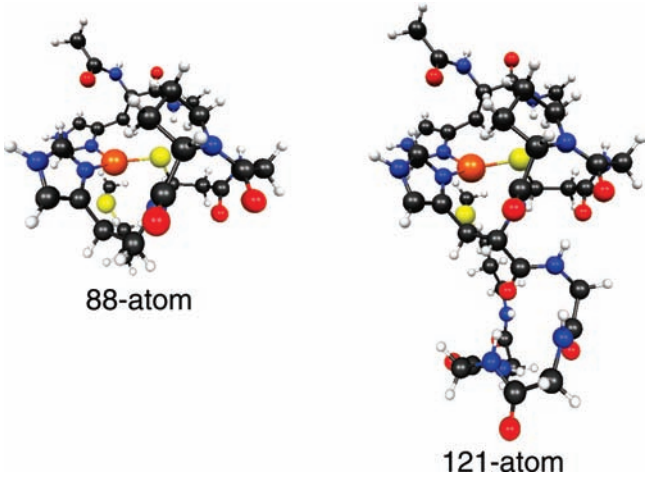

Figure 1. 88-atom and 121-atom model molecules extracted from the X-ray structure 1KDI (H atoms are added).

method, protein matrix and aqueous solvation to the model molecules is treated in an efficient way.

II. Computational Methodology

All electronic structure calculations were performed with the GAMESS program.[50,51]

The X-ray structures were obtained from the protein data bank (PDB).[52] Hydrogen atoms were added to the structures using the WHAT IF web interface.[53] Active site model molecules (Figures 1, 2, 3, and 4) were extracted from these X-ray structures and edited by manually deleting unwanted atoms and adding new hydrogen atoms to fill the open bonds.

To determine the minimum model size and the minimum number of atoms to be optimized, active site model molecules consisting of 88 atoms and 121 atoms were extracted from 13 X-ray structures for 11 plastocyanins (Table 1, Figure 1). Plastocyanin is a typical small type-1 Cu protein consisting of ~100 amino acid residues. Despite the differences in the amino acid sequences, the overall 3D folding of all the 11 plastocyanins considered in this study are similar. The similarity of their type-1 Cu centers is even higher: they possess identical ligands and exhibit almost the same local 3D structures and very similar E^0 (all around 370 mV), implying that the protein matrices have very little effect on the E^0. Chemically identical active sites consisting of up to 130 atoms for these type-1 Cu centers can be isolated from these plastocyanins. This allows one to focus on the local structural factors and short-range interactions without necessarily considering the long-range interactions from the rest of the protein. Geometry optimizations were performed in the gas phase with RHF[54] and ROHF[55] methods, respectively, for the Cu^+ and Cu^{2+} oxidation states of these model molecules. The 6-31G* basis set[56,57] was used. For the 88-atom models, the coordinates of 0, 8, 29, 41, and 67 atoms were optimized; for the 121-atom models, the coordinates of 0 and 61 atoms were optimized. These model molecules are denoted as 88-0, 88-8, 88-29, 88-41, 88-67, 121-0 and 121-61 models (Table 2, Figure 2). In Figure 2, red atoms are optimized while blue atoms are fixed in their X-ray coordinates.

In the calculation of E^0 for type-1 Cu centers in cucumber stellacyanin, D.c. plastocyanin, M148Q T.f. rusticyanin, T.f. rusticyanin, and M148L T.f. rusticyanin, active site model molecules consisting of ~100 atoms were extracted from the X-ray structures 1JER,[58] 1KDI,[59] 1E30,[60] 2CAK,[61] and 1GY2[62] (Figures 3 and 4). For each model molecule, the coordinates of

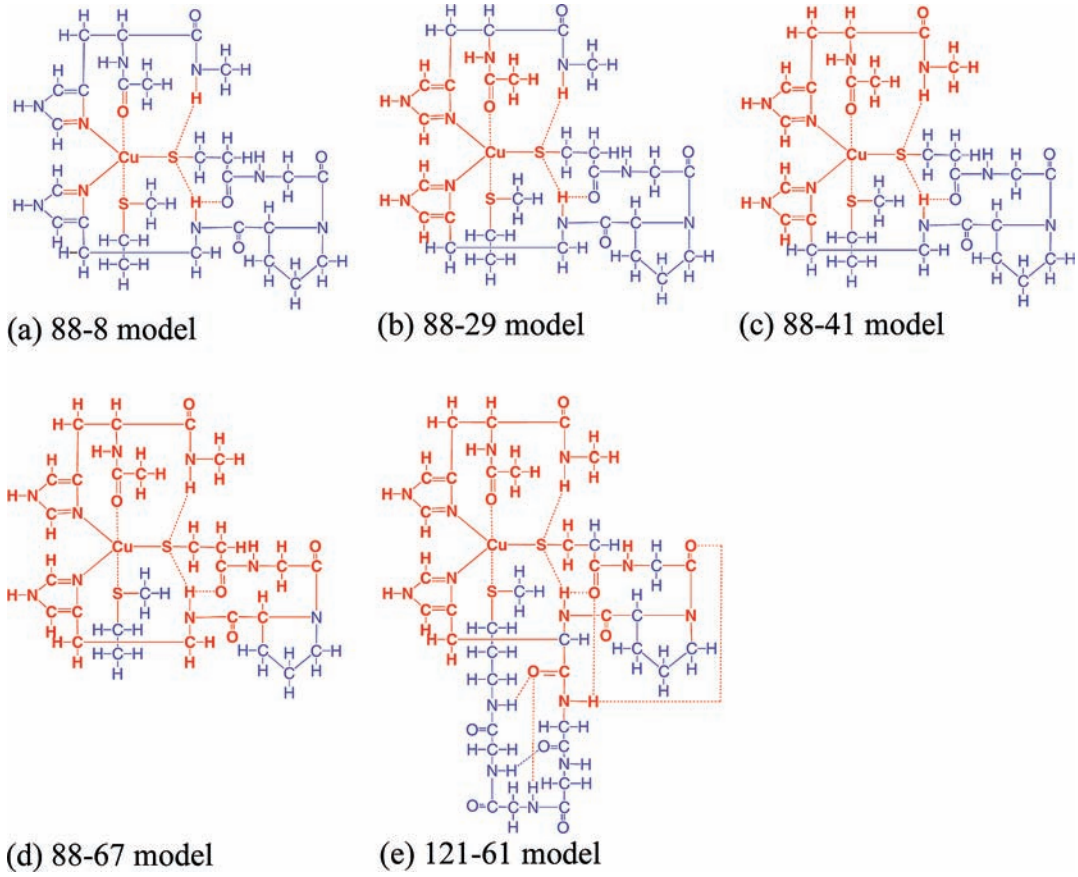

Figure 2. 88-atom and 121-atom model molecules for plastocyanins. Red atoms are optimized while blue atoms are fixed.

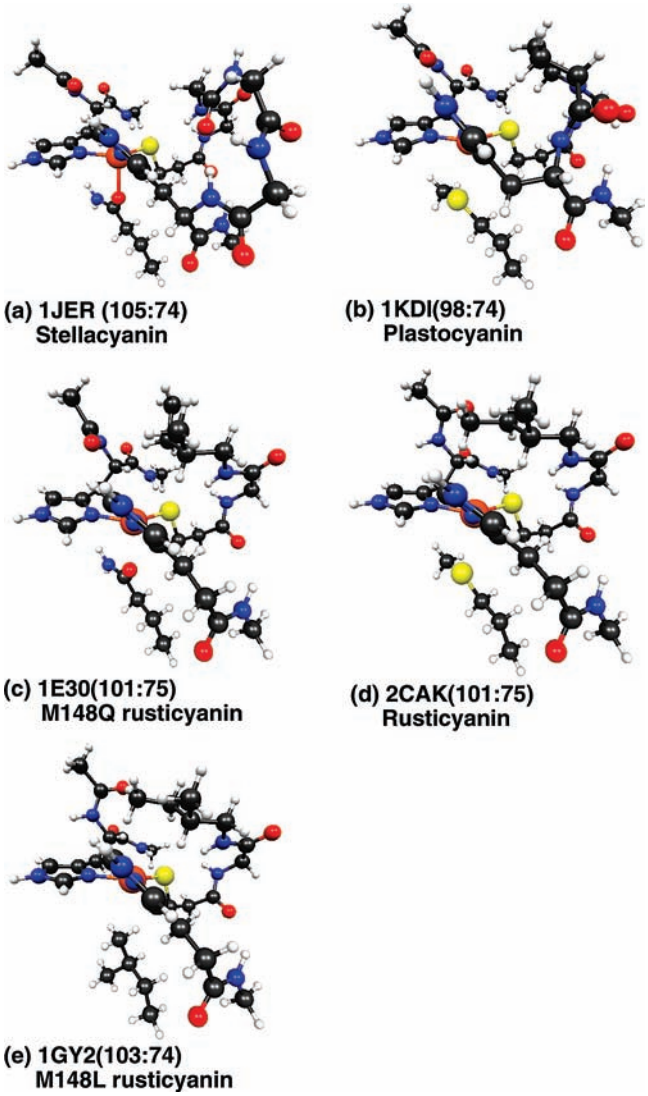

Figure 3. Model molecules of five type-1 Cu centers extracted from X-ray crystal structures. The numbers of total and optimized atoms are indicated in parentheses.

~70 atoms were optimized with the CPCM[46,63,64]/B3LYP[47]/6-31G* method, with the R-B3LYP and RO-B3LYP type of wave function for Cu^+ and Cu^{2+}, respectively. In order to mimic the forces imposed by the protein, ~30 atoms were fixed in their X-ray coordinates. In Figure 4, red atoms are optimized while blue atoms are fixed, and the numbers of total and optimized atoms are indicated after the PDB names.

Two CPCM methods were used. One is the usual homogeneous CPCM (Homo-CPCM,[63,64] an approximation of the more rigorous and accurate IEF-PCM[34,35]) in which only one dielectric constant is used to describe a homogeneous and isotropic solvent, such as bulk water. The other is a recently developed heterogeneous CPCM (Het-CPCM[46]) in which different local effective dielectric constants can be defined for different surface regions to represent a heterogeneous environment, such as an active site solvated by protein matrix and bulk water. Practically, this is realized by defining different effective dielectric constants for different spheres used to form the solute cavity. In the current implementation, the CPCM boundary elements or tesserae on the same sphere have the same dielectric constant. The Het-CPCM has been implemented for energy and analytic gradient calculation. Both the Homo- and Het-CPCM calculations (energy and gradients) are very efficient, and only add a few percent of computing time to the corresponding gas phase calculations for a molecule consisting of ~100 atoms. The details of the Het-CPCM can be found in ref 46.

In both the Homo-CPCM and Het-CPCM methods, spheres with radii of 2.124, 2.016, 1.908, 2.52, and 2.76 Å were used for C, N, O, S, and Cu atoms, respectively, to define the molecular cavity. The FIXPVA tessellation scheme[65] was used with 60 initial tesserae per sphere. No charge renormalization was performed, and only the CPCM electrostatic interaction was calculated as the solvation free energy.

In the Homo-CPCM method, a dielectric constant of 78.39 was used. In the Het-CPCM calculations, spheres associated with solvent-exposed atoms are assigned with a dielectric constant of 78.39. His143 is the solvent-exposed group in the 1E30, 2CAK, and 1GY2 model molecules; most of the atoms in the 1JER and 1KDI model molecules are solvent-exposed, with 23 and 15 atoms, respectively, being buried (Figure 4). The spheres associated with atoms embedded in the protein are assigned with lower dielectric constants: 4 for rusticyanin and 20 for stellacyanin and plastocyanin.

Using dielectric constants between 4 and 20 is reasonable because they have been commonly used for proteins. Experiments[66–68] show that the dielectric constants of "dry protein powders" are ~1.2, and those of "water-adsorbed protein powders" are typically 2−5, depending on the protein and the weight fraction of adsorbed water. Therefore, many continuum electrostatic studies used 2−4 for protein interiors. However, sophisticated theoretical studies performed by Warshel and coworkers (for example, King et al.[69]) suggest that the dielectric constants of protein interiors are dependent on the bulk solvent, and some protein active sites show higher values such as 10 when solvent reaction field is considered. Large values such as 20 could also exist due to solvent effect. In continuum electrostatics pK_a calculations, which are most relevant to the E^0 calculations in the current study, Antosiewicz et al. found that the best overall results can be obtained if $\varepsilon = 20$ is used.[70] They also noted that protein interiors should have dielectric constants smaller than 20. Therefore, protein interior dielectric constants are most likely 4−10 and can be as large as 20.

An inspection of the protein environments around the type-1 Cu centers shows that the degree of burial of the type-1 Cu centers is lower for cucumber stellacyanin (1JER) and D.c. plastocyanin (1KDI) as compared to that for rusticyanin. A previous empirical study on protein pK_a (PROPKA[71]) has found that the number of protein C, N, O atoms within ~15.5 Å to a pK_a site can be used to describe the desolvation effect on pK_a shift. In principle, such numbers can also be used to estimate the desolvation effect on E^0. The numbers of protein C, N, O atoms within 15.5 Å to the Cu ions in the PDB files are 453, 445, 536, 512, and 515, respectively, for 1JER, 1KDI, 1E30, 2CAK, and 1GY2. Clearly, the Cu ions in cucumber stellacyanin (1JER) and D.c. plastocyanin (1KDI) are less buried (i.e., more solvated), and those in rusticyanin (1E30, 2CAK, and 1GY2) are more buried (i.e., less solvated). A nuclear magnetic resonance study suggests that the protein matrix around the rusticyanin type-1 Cu center is highly hydrophobic and rigid, which corresponds to a low effective dielectric constant.[72] To minimize the arbitrariness, the high-end value $\varepsilon = 20$ was used for 1JER and 1KDI, and the low-end value $\varepsilon = 4$ was used for 1E30, 2CAK, and 1GY2. One must keep in mind that the accurate effective dielectric is unknown and could be significantly different at different portions around the type-1 centers. In general, determining protein interior dielectric is a difficult issue.[18]

Based on the Homo- and Het-CPCM/B3LYP/6-31G* optimized structures, single-point energies were calculated using Homo- and Het-CPCM/B3LYP methods with a mixed triple-ζ basis set: the standard 6-311++G(2df,p)[73] for H, C, N, O, and S and cc-pVTZ[74] for Cu. Using such a large basis set is necessary for accurate description of the Cu−ligand interactions in which polarization has significant contributions (see section III for discussions). Using the mixed triple-ζ basis set means ~2300 basis functions for each model molecule. In the CPCM calculations with these basis sets, approximately 0.05−0.06 e of electronic charge is distributed outside of the CPCM cavity. Since it is almost a constant in all the model molecules, such charge leaking is unlikely to cause significant differences in the calculated E^0.

A relative method is used to calculate E^0. For a given type-1 Cu protein (Pro) and a reference type-1 Cu protein (Ref), the free energy change for the following electron transfer reaction

$$\text{ProCu(II)} + \text{RefCu(I)} \xrightarrow{\Delta G} \text{ProCu(I)} + \text{RefCu(II)} \qquad (1)$$

is approximated with the electronic energy (including nuclear repulsion and solvation free energy) computed for the model molecules

$$\Delta G \approx \Delta G^{\text{ele}} = \Delta G^{\text{ele}}_{\text{ProCu(I)}} + \Delta G^{\text{ele}}_{\text{RefCu(II)}} - \Delta G^{\text{ele}}_{\text{ProCu(II)}} - \Delta G^{\text{ele}}_{\text{RefCu(I)}} \qquad (2)$$

The relative method is based on the assumption that the differences in the zero-point energies, thermal energies, and entropies of the model molecules make minor contributions to the relative E^0. This is indeed a good approximation when a

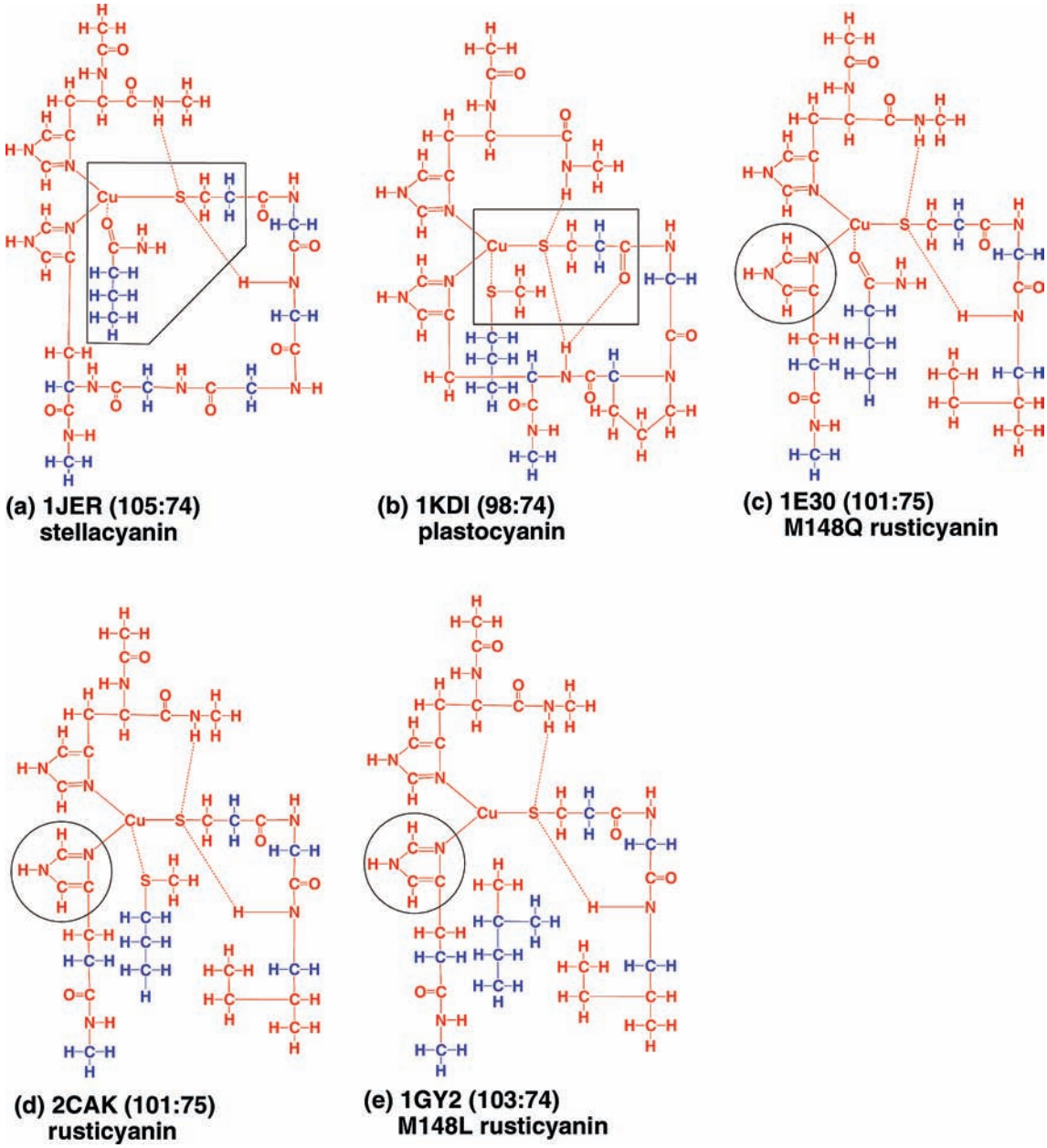

Figure 4. Model molecules of five type-1 Cu centers extracted from X-ray crystal structures. Red atoms are optimized while blue atoms are fixed (the numbers of total and optimized atoms are indicated after the PDB names). In Het-CPCM calculations, spheres associated with solvent-exposed atoms (noncycled atoms for 1JER and 1KDI, cycled atoms for 1E30, 2CAK, and 1GY2) are assigned with $\varepsilon = 78.39$ while the spheres associated with protein-buried atoms are assigned with smaller dielectric constants: $\varepsilon = 20$ for 1JER and 1KDI, $\varepsilon = 4$ for others.

TABLE 1: Thirteen Plastocyanin X-ray Structures

PDB	species	O.S.	E^0 (mV)	E^0 ref
1KDI[59]	fern dryopteris crassirhizoma (*Adiantum capillus-veneris*)	Cu^+	376	75
2BZ7[75]	fern dryopteris crassirhizoma (*A. capillus-veneris*), G36P	Cu^{2+}	363	75
2BZC[75]	fern dryopteris crassirhizoma (*A. capillus-veneris*), G36P	Cu^+	363	75
5PCY[91]	poplar (*Populus nigra*)	Cu^+	370	90
1PNC[92]	poplar (*P. nigra*)	Cu^{2+}	370	90
1JXG[93]	poplar (*P. nigra*), I21C, E25C	Cu^{2+}	348	93
2CJ3[94]	cyanobacterium (*Anabaena variabilis*)	Cu^{2+}	360	95
1BXU[96]	cyanobacterium (*Synechococcus* sp.) pcc 7942	Cu^{2+}	370	*a*
1PCS[97]	cyanobacterium (*Synechocystis* sp.) pcc 6803, A42D, D47P, A63L	Cu^{2+}	325	97
7PCY[98]	green alga (*Enteromorpha prolifera*)	Cu^{2+}	369	90
2PLT[99]	green alga (*Chlamydomonas reinhardtii*)	Cu^{2+}	370	*a*
1AG6[100]	spinach (*Spinacia oleracea*), G8D	Cu^{2+}	379	100
1IUZ[101]	sea lettuce (*Ulva pertusa*)	Cu^{2+}	363	102

[a] The E^0 was not found in the literature by the authors, and a value of 370 mV is estimated.

TABLE 2: E^0 (mV) Calculated with the Gas Phase RHF/6-31G* and ROHF/6-31G* Methods for Plastocyanin Using 13 X-ray Structures

model	88-0	88-8	88-29	88-41	88-67	121-0	121-61	expt
1KDI	376	376	376	376	376	376	376	376
7PCY	322	308	317	306	414	315	365	369
5PCY	619	216	382	336	409	658	413	370
1AG6	−24	−12	202	220	389	−25	327	379
1PCS	−18	−94	151	171	403	−35	280	325
1PNC	138	197	226	231	407	154	336	370
2BZC	393	271	421	395	402	416	433	363
2BZ7	380	232	398	371	411	372	378	363
1IUZ	288	263				315	349	363
2CJ3	193	184				274	449	360
1JXG	103	87				146	373	348
2PLT	54	18				79	323	370
1BXU	28	−50				66	369	370
max unsigned error	403	420	177	159	78	404	89	
mean unsigned error[a]	206	228	93	84	42	193	37	

[a] 1KDI excluded.

series of similar protein active sites are considered. The free energy contributions due to the protein matrix and aqueous solvent are included in the CPCM solvation free energy.

The E^0 of the protein at $T = 298.15$ K is computed by

$$E^0_{Pro} = E^0_{Ref} + \Delta G/F \quad (3)$$

where F is the Faraday constant and E^0_{Ref} is the experimental E^0 of the reference type-1 Cu protein (relative to standard hydrogen electrode). For the 11 plastocyanins, the fern plastocyanin (1KDI model) is used as the reference. For the five type-1 Cu centers, the rusticyanin (2CAK model) is used as the reference.

III. Results and Discussion

A. Structural Sensitivity. Table 2 presents the E^0 calculated with RHF/6-31G* and ROHF/6-31G* methods for the 13 X-ray structures. The experimental E^0 values of the plastocyanins are also listed for comparison. Fern plastocyanin[75] (X-ray structure 1KDI[59] in PDB), which has $E^0 = 376$ mV relative to standard hydrogen electrode, is used as the reference. The E^0 for *Cyanobacterium pcc 7942* (1BXU) and green alga (*Chlamydomonas reinhardtii*) plastocyanin (2PLT) were not found from the literature by the authors, and 370 mV was estimated.

With no geometry optimization (88-0 and 121-0 models) or very limited geometry optimization (88-8 models), the relative E^0 values calculated with the gas phase RHF/6-31G* and ROHF/6-31G* energies show maximum errors of ~400 mV and mean errors of ~200 mV. In going from the 88-8 models to the 88-29 models, the E^0 values are significantly improved, resulting in a maximum unsigned error = 177 mV and a mean unsigned error = 93 mV. Very small changes are observed for all the eight cases in going from 88-29 models to 88-41 models: the errors for 7PCY, 5PCY, 2BZC, and 2BZ7 are still small (<63 mV), and the errors for 1AG6, 1PCS, and 1PNC are still large (>139 mV), leaving a maximum error = 159 mV and a mean error = 84 mV. Although the calculated E^0 values are seemingly good (max error = 78 mV and mean error = 42 mV), the 88-67 models have intrinsic problems: so many atoms are relaxed that the structures are significantly different from the experimental X-ray structures. Therefore, the 88-67 models are not good models for the proteins and should not be used. However, they suggest that ~60 or more atoms should be optimized in order to reduce the E^0 errors caused by the structural errors to below 100 mV.

In order to relax the type-1 Cu centers while keeping the structures of the model molecules similar to the protein structures, model molecules with more than 88 atoms shall be used to include more protein interactions and constraints. The 121-atoms model molecules are therefore studied. Figure 2e shows the 61 atoms optimized in the 121-61 models. As expected, a max error = 89 mV and a mean error = 37 mV are obtained.

To summarize, the calculated relative E^0 values are very sensitive to the geometry optimization of the model molecules. Therefore, relatively large (e.g., 100 atoms) model molecules should be used, and a sufficient number (e.g., 60) of atoms

TABLE 3: Het-CPCM/B3LYP/6-31G* Optimized Cu−Ligand Distances (Å) in the Model Molecules

species	PDB	Cu−S(Cys)		Cu−N(His1)[a]		Cu−N(His2)[b]		Cu−axial[c]	
		Cu^{2+}	Cu^{+}	Cu^{2+}	Cu^{+}	Cu^{2+}	Cu^{+}	Cu^{2+}	Cu^{+}
cucumber stellacyanin	1JER	2.221	2.288	1.965	2.018	1.947	1.970	2.097	2.181
D.c. plastocyanin	1KDI	2.236	2.290	1.975	1.982	1.964	2.011	2.467	2.613
M148Q T.f. rusticyanin	1E30	2.218	2.285	1.969	1.979	1.943	2.003	2.114	2.204
T.f. rusticyanin	2CAK	2.217	2.326	1.993	2.001	1.962	2.008	2.536	2.499
M148L T.f. rusticyanin	1GY2	2.152	2.254	1.956	1.989	1.942	1.970	2.924	3.012

[a] N-terminal His. [b] C-terminal His. [c] Cu−S(Met) in 1KDI and 2CAK, Cu−O(Gln) in 1JER and 1E30, Cu−C(Leu) in 1GY2.

should be optimized. This guideline is used in the following studies of five type-1 Cu centers.

B. Cu−Ligand Distances. The Cu−ligand distances in the Het-CPCM/B3LYP/6-31G* optimized model molecules for cucumber stellacyanin, D.c. plastocyanin, Met148Gln, Met148Leu, and wild-type T.f. rusticyanin are listed in Table 3. The Homo-CPCM/B3LYP/6-31G* results are very similar, thus not listed.

The Cu−S^{-}(Cys) and Cu−N(His) bonds are strong and rigid and show small variations in different model molecules. The optimized Cu^{2+}−S^{-}(Cys) distances vary from 2.15 to 2.23 Å, and Cu^{+}−S^{-}(Cys) distances vary from 2.25 to 2.33 Å. The Cu^{2+}−N(His) distances vary from 1.94 to 1.99 Å, with the C-terminal N(His) distances always shorter than the N-terminal N(His) distances by 0.01−0.03 Å. The Cu^{+}−N(His) distances vary from 1.97 to 2.02 Å, with the C-terminal N(His) distances either shorter or longer than the N-terminal N(His) distances by 0.01−0.05 Å.

The Cu^{2+}−O(Gln) distances in 1JER and 1E30 models are 2.097 and 2.114 Å, while the Cu^{+}−O(Gln) distances are 2.181 and 2.204 Å, as compared to 2.21 and 2.33 Å in the X-ray structures.

The Cu^{2+}−S(Met) distances in 1KDI and 2CAK models are 2.467 and 2.536 Å, while the Cu^{+}−S(Met) distances are 2.613 and 2.499 Å, respectively, shorter than the 2.91−2.92 Å in the X-ray structures. Geometry optimization of smaller type-1 Cu model molecules performed by the author's group using the second-order perturbation theory method (MP2) gives similarly short distances [∼2.6 Å for Cu^{2+}−S(Met) and ∼2.3 Å for Cu^{+}−S(Met)], so it is unlikely that the short distances are due to errors in the B3LYP method. Instead, it is an intrinsic property of the $Cu^{2+/+}$−S(Met) bonds. This has been noticed and discussed in the literature for a long time, for example, by Ryde,[76] Solomon,[77] and Ando.[78] Recent experimental results[79] from Solomon's group show that the axial Cu−S(Met) distance is not constrained in nitrite reductase, so it can take two possible values, 2.4 and 4.3 Å. The constant Cu−S(Met) distances of ∼2.9 Å in plastocyanin and rusticyanin crystals are presumably due to interactions from other groups or packing forces. As shown in Figure 4, many atoms of the Met ligand were fixed during geometry optimization, but the resultant Cu−S(Met) distances are still too short in the 1KDI and 2CAK models. Therefore, such protein interactions are most likely intermolecular interactions instead of covalent bond forces. The details of these interactions are currently unknown. The author's group is using the MP2 method and realistic models to probe these protein interactions. In subsection D, the potential errors in the computed E^0 due to the shortened Cu−S(Met) distances will be discussed.

C. Solvation Effect. Using the Het-CPCM/B3LYP/6-311G(2df,p) method, the calculated relative E^0 values for cucumber stellacyanin, D.c. plastocyanin, Met148Gln, Met148Leu, and wild-type T.f. rusticyanin are 242, 366, 522, 667, and 825 mV, respectively, which compare well to experiment values 260, 376, 563, 667, and 798 mV (Table 4). The maximum unsigned error is 41 mV, with a mean unsigned error of 24 mV (2CAK excluded).

TABLE 4: Calculated Reduction Potential E^0 (mV) for Five Type-1 Cu Centers

species	Homo/DZ[a]	Homo/TZ[b]	Het/DZ[c]	Het/TZ[d]	expt[e]
cucumber stellacyanin	333	480	158	242	260
D.c. plastocyanin	554	616	367	366	376
M148Q T.f. rusticyanin	381	501	456	522	563
T.f. rusticyanin	667	667	667	667	667
M148L T.f. rusticyanin	843	849	832	825	798

[a] Homo-CPCM/B3LYP/6-31G*. [b] Homo-CPCM/B3LYP/6-311++G-(2df,p)//Homo-CPCM/B3LYP/6-31G*. [c] Het-CPCM/B3LYP/6-31G*. [d] Het-CPCM/B3LYP/6-311++G(2df,p)//Het-CPCM/B3LYP/6-31G*. [e] For stellacyanin and plastocyanin, pH ∼ 7; for rusticyanins, pH = 3.2. See text for discussion.

The experimental values[75,80] for stellacyanin and plastocyanin were measured at pH ∼ 7, and the values[60] for rusticyanins were measured at pH = 3.2. Indeed, the E^0 of rusticyanins changes significantly in going from pH = 7 to pH = 3.2.[60] According to Giudici-Orticoni et al., the pK_a value of the N^{δ} proton of the solvent-exposed His143 imidazole is ∼7 for Cu^{2+} rusticyanin.[81] The pK_a value of the N^{ε} proton of His143 imidazolium should be much lower than 2.[82,83] So, at pH ∼ 3, it is a neutral imidazole coordinating to the $Cu^{2+/1+}$ ions and the E^0 is ∼680 mV, while at pH∼7, it is an imidazolate anion coordinating to the $Cu^{2+/1+}$ ions and the E^0 is ∼550 mV. Such a change in E^0 is apparently due to the charge−charge interaction between the proton and $Cu^{2+/+}$ ions. This study intended to calculate the E^0 at pH 2−3, the natural state of this protein, and used model molecules with neutral imidazoles for the three rusticyanins (Figures 3 and 4). Therefore, the computed E^0 should be compared to the experimental E^0 at pH ∼ 3.

Using the Homo-CPCM/B3LYP/6-311++G(2df,p) method with $\varepsilon = 78.39$, the calculated relative E^0 values (480 and 616 mV) for cucumber stellacyanin and D.c. plastocyanin are too high as compared to experimental values 260 and 376 mV (at pH ∼ 7).[75,80] This is not surprising because it is intrinsically wrong to use the same dielectric constant to describe the heterogeneous and different environments surrounding the model molecules.

The model molecules for stellacyanin (1JER) and Met148Gln rusticyanin (1E30) both have two H-bonds to S^{-}(Cys) and the same axial O(Gln) ligand, so they have almost the same E^0, 480 versus 501 mV, when the Homo-CPCM method is used. The model molecules for plastocyanin (1KDI) and rusticyanin (2CAK) both have two H-bonds to S^{-}(Cys) and the same axial S(Met) ligand, so they have similar E^0, 616 versus 667 mV, with a 51 mV difference mainly caused by the difference in the strength of the H-bonds to the S^{-}(Cys) ligands (see subsection E).

Clearly, the solvation effects introduced by using $\varepsilon = 4$ for protein-buried atoms in rusticyanins (1E30, 2CAK, and 1GY2) and $\varepsilon = 20$ for protein-buried atoms in stellacyanin (1JER) and plastocyanin (1KDI) can create ∼250 mV differences in E^0.

How the bulk water and protein matrix solvation affects the E^0 of the type-1 Cu center can also be understood by examining the absolute E^0 computed for rusticyanin (2CAK model). Using the homogeneous CPCM($\varepsilon = 78.39$)/B3LYP/6-31G* optimized structure and energy, the energy difference is 81.29 kcal/mol or 3525 mV; using the heterogeneous CPCM/B3LYP/6-31G* optimized structure and energy, the energy difference is 85.79 kcal/mol or 3720 mV. Therefore, in rusticyanin the protein burial can likely raise the reduction potential by ~200 mV. This value is similar to the ~250 mV difference between rusticyanin and stellacyanin or plastocyanin.

In the current study arbitrariness has not been avoided due to the author's selection of the effective dielectric constants. Therefore, the results obtained with the Het-CPCM method should be regarded as a semiquantitative estimation of the desolvation effects on E^0.

Permanent electrostatic interactions from the protein matrix are not considered in the current work. A comparison to calculations using electrostatic models will be presented in subsection F.

D. Axial Ligands. It is well-known that axial ligands can preferentially stabilize Cu^{2+} and thus decrease the E^0. For example, the Met148Gln, native, and Met148Leu rusticyanins have E^0 values of 563, 667, and 798 mV, respectively.[60] The E^0 values calculated with the Het-CPCM/B3LYP/6-311++G(2df,p) method are 522, 667, and 825 mV, respectively, in good agreement with the experimental values 563, 667, and 798 mV (Table 4). The Homo-CPCM/B3LYP/6-311++G(2df,p) method gives slightly worse results, 501, 667, and 849 mV, respectively (Table 4).

A very similar case is the Gln99Met, Gln99Leu, and wild type stellacyanin, for which the S(Met) and O(Gln) ligands are able to decrease the E^0 by ~160 and ~320 mV, respectively, as compared to Leu.[80,84]

In a study of $Cu^{2+/+}$−ligand interaction using B3LYP, MP2, CCSD, and CCSD(T) methods performed by the author's group,[85] it is found that for Cu^+−water, Cu^+−imidazole, Cu^+−$S^-(CH_3)$, and Cu^+−$S(CH_3)_2$, all in equilibrium geometries, B3LYP tends to overestimate the interaction energies by ~2, ~4, ~7, and ~5 kcal/mol as compared to coupled cluster singles, doubles with noniterative triples [CCSD(T)] method; for Cu^{2+}−water, Cu^{2+}−imidazole, Cu^{2+}−$S^-(CH_3)$, and Cu^{2+}−$S(CH_3)_2$, B3LYP tends to overestimate the interaction energies by ~11, ~18, ~24, and ~25 kcal/mol as compared to the coupled cluster singles, doubles (CCSD) method. In the current study, the large errors in the $Cu^{2+/+}$−S^-(Cys) and $Cu^{2+/+}$−N(His) interactions are canceled because all the model molecules have similar Cu−S−N−N core structures. Although it is not clear how much B3LYP will overestimate the axial $Cu^{2+/+}$−O(Gln) and $Cu^{2+/+}$−S(Met) interactions in the model molecules when the Cu ions are already strongly coordinated by the equatorial S^-(Cys) and N(His) ligands and a continuum solvation model is used, the magnitude of the overestimation should be very smaller, such as ~1 kcal/mol or ~40 mV. Indeed, the Het-CPCM/B3LYP/6-311++G(2df,p) predicted E^0 values for Met148Gln and wild type Met148 rusticyanin (relative to Met148Leu rusticyanin) are ~41 and ~27 mV too low as compared to experimental values. As discussed above, the Cu−S(Met) distance in the 2CAK model is ~2.5 Å as compared to ~2.9 Å in the X-ray structure 2CAK. This shortening may also contribute to the overestimation of the E^0 change in going from Met148Leu rusticyanin to wild type Met148 rusticyanin.

The standard 6-31G* basis set is insufficient for modeling electron density polarization, which is crucial in determining the relative coordination strength of Cu to the CH_3(Leu), S(Met), and O(Gln) ligands. For example, for the three rusticyanins, the relative E^0 values calculated with Het-CPCM/B3LYP/6-31G* are 456, 667, and 832 mV, respectively, worse than the 6-311++G(2df,p) results. Similar basis set effects can be seen for cucumber stellacyanin, for which the Het-CPCM/B3LYP calculated E^0 is improved by 84 mV in going from 6-31G* to 6-311++G(2df,p). It is also interesting to note that the basis set error is larger when the Homo-CPCM method is used. For example, the E^0 values calculated for Met148Gln with the Homo- and Het-CPCM/B3LYP/6-31G* methods are 381 and 456 mV, respectively, as compared to the experimental value 563 mV (Table 4). It is well-known that triple-ζ quality basis sets can usually converge B3LYP calculated relative energies to within ~1 kcal/mol. Therefore, larger basis sets were not attempted. Using GAMESS, open-shell B3LYP calculations for metal systems are difficult to converge when large basis sets are used.

It must be emphasized that the good agreement between the calculated and experimental axial ligand interactions is contingent on the Het-CPCM solvation effect. For example, the E^0 difference between native and Met148Leu rusticyanins computed with the gas phase B3LYP/6-311++G(2df,p) method is 248 mV, much larger than the 158 mV from Het-CPCM/B3LYP/6-311++G(2df,p) and the 131 mV from experiments. This observation suggests that using a continuum solvation model to describe the rusticyanin protein matrix is quite a good approximation. The gas phase data for Met148Gln rusticyanin are not available for comparison because the SCF calculation did not converge. A recent computational study on His143Met, Met148Gln, and wild type rusticyanins show that gas phase results overestimate experimental mutagenesis E^0 changes, while QM/MM methods tend to slightly underestimate.[61]

E. Hydrogen Bonding to S^-(Cys). Hydrogen bonding to the Cu-bound S^-(Cys) ligand can raise the E^0. Experimental mutagenesis of A.f. pseudoazurin shows that the Pro80Ala and Pro80Ile variants have one more backbone hydrogen bond to the copper-bound S^-(Cys) than the wild type does and show 139 and 180 mV higher E^0, respectively.[12] Similarly, the Pro94Ala and Pro94Phe mutants of P.d. amicyanin have higher E^0 than the wild type 115 and 150 mV, respectively, due to the creation of a new hydrogen bond to the copper-bound S^-(Cys).[86]

The 51 mV difference in the Homo-CPCM/B3LYP/6-311++G(2df,p) calculated E^0 for plastocyanin (1KDI, 616 mV) and rusticyanin (2CAK, 667 mV, the reference) is likely caused by the second hydrogen bond to the S^-(Cys) ligands, which is weaker in 1KDI but stronger in 2CAK. In the optimized oxidized form of the 2CAK model molecule, there are two similar backbone amide hydrogen bonds to the S^-(Cys), with S−H distances of 2.64 and 2.66 Å and S−H−N angles of 168°and 169°, respectively. In the optimized oxidized form of the 1KDI model molecule, the two S−H distances are 2.51 and 2.84 Å, and the two S−H−N angles are 177°and 152°, respectively, suggesting that there are two hydrogen bonds; one is strong and one is weak. This effect cannot be obviously seen in the Het-CPCM results because these two models used very different dielectric constants for protein-buried regions, and the 1KDI model gains an additional E^0 lowering of 250 mV due to the solvation effects.

F. Comparison to Previous Calculations. A few computational studies on calculating E^0 of type-1 Cu centers are in the literature. A comparison of the current work with them is presented below.

Olsson and Ryde[19] calculated relative E^0 for type-1 Cu centers in stellacyanin, plastocyanin, azurin, rusticyanin, and ceruloplasmin with the B3LYP and PCM method and model molecules consisting of ~50 atoms. Their main purpose is to elucidate the influence of the axial ligands such as Met and Gln on E^0. They performed full and constrained geometry optimizations and concluded that axial ligand interactions can affect the E^0, similar to the results from the current work. Compared to their method, the current work used larger and more realistic model molecules, so some protein interactions are included. In addition, protein matrix and bulk solvation to the active sites were modeled more accurately with the Het-CPCM method, while Olsson and Ryde only used Homo-PCM to estimate aqueous solvent effect.

Botuyan et al.[17] calculated the relative reduction potentials for French bean plastocyanin and rusticyanin using a continuum electrostatic model. The E^0 differences obtained with NMR structures and X-ray structures are 228 and 389 mV, respectively. Their results suggest that the E^0 differences are caused by both hydrophobicity in rusticyanin and some specific charge−charge and charge−dipole interactions. Jimenez et al.[72] performed a nuclear magnetic resonance study for rusticyanin and concluded that its high hydrophobicity and rigidity are responsible for its high E^0. Using protein dipole/Langevin dipole and QM/MM frozen density functional free energy simulation techniques, Olsson, Hong, and Warshel[20] predicted similar values for poplar plastocyanin and rusticyanin (300 mV) and suggested that the E^0 differences between plastocyanin and rusticyanin are caused by many small protein dipole interactions with the Cu ions. In the current work, permanent electrostatic interactions from the protein matrix are not considered. If the hydrophobicity in rusticyanin is not considered, the calculated E^0 values for plastocyanin and rusticyanin are similar, 616 versus 667 mV, as shown in Table 4. If the hydrophobicity is considered, the calculated E^0 values are 366 versus 667 mV (Table 4). Therefore, the current study suggests that hydrophobicity is the main cause of the high E^0 of rusticyanin, in accordance with Jimenez et al.'s results[72] and in partial agreement with Botuyan et al.'s results.[17]

In an earlier work Li et al.[21] studied the structural determinants of the E^0 for six type-1 Cu proteins, cucumber stellacyanin, P.a. azurin, poplar plastocyanin, C.c. laccase, T.f. rusticyanin, and human ceruloplasmin. Chemical models consisting of ~100 atoms for the type-1 Cu centers were extracted from X-ray structures. Two major structural determinants, Cu ligands and hydrogen bonds to the Cu-bound S_{Cys}, were examined by comparing the E^0 of successively simpler models. However, the effect of structure relaxation of the active sites was not fully examined (only a few atoms were optimized), and considerably large errors were in the calculated relative E^0 for different species. In addition, only the 6-31G* basis set was used at that time due to the limit of computing power. Considering geometry relaxation, recent calculations suggest that solvation effect must be considered in order to explain the large E^0 range of type-1 Cu centers in different species (to be published[87]). The major improvements in the current study are the use of Het-CPCM, which has been developed recently and shown to be more realistic and accurate, and the use of the B3LYP method and the 6-311++G(2df,p) basis set, which are more accurate than the HF/6-31G* method.

IV. Conclusion

Results of this work show that type-1 Cu reduction potentials (E^0) calculated with quantum chemical methods are very sensitive to the structures of the model molecules. In order to minimize the errors caused by the differences in the X-ray structures, relatively large (e.g., 100 atoms) model molecules should be used and a sufficient number (e.g., 60) of atoms should be optimized. Using model molecules consisting of ~100 atoms, the E^0 of five type-1 Cu centers in cucumber stellacyanin, D.c. plastocyanin, Met148Gln rusticyanin, wild type rusticyanin, and Met148Leu rusticyanin were calculated with a heterogeneous conductor-like polarizable continuum model (Het-CPCM) incorporated in the B3LYP method as a reaction field. The Het-CPCM/B3LYP/6-311++G(2df,p) [cc-pVTZ for Cu] calculated E^0 values are 242, 366, 522, 667, and 825 mV, respectively, in good agreement with experimental values 260, 376, 563, 667, and 798 mV (Table 4). The very high E^0 (798 mV) for Met148Leu rusticyanin (1GY2) is mainly due to the lack of the axial ligand, and two hydrogen bonds to the Cu-bound S^-(Cys) ligand, as well as the hydrophobic and rigid environment around the type-1 Cu center. Compared to Met148Leu rusticyanin, wild type rusticyanin (2CAK) has an axial S(Met) ligand, which brings the E^0 down to 667 mV. The axial O(Gln) ligand in Met148Gln rusticyanin (1E30) is the main cause of its 563 mV E^0. The type-1 Cu center in stellacyanin (1JER) is very similar to that in Met148Gln rusticyanin but is much more solvated by the aqueous solvent. The type-1 Cu center in plastocyanin (1KDI) is similar to that in wild type rusticyanin, but with a slightly weaker hydrogen bond to the S^-(Cys) ligand, and is much more solvated by the aqueous solvent. According to the Het-CPCM calculations, the difference in the solvation energy can likely create a difference of ~250 mV in the E^0. Mainly due to these reasons, stellacyanin and plastocyanin show much lower E^0 values, 260 and 376 mV. Therefore, ligand interaction (~250 mV) and solvation effect (~250 mV) are the main determinants of the relative E^0 of these five type-1 Cu centers, as has been proposed by Malmström, Solomon, and Gray.[88–90]

Acknowledgment. This work was supported by startup funds from the University of Nebraska—Lincoln.

References and Notes

(1) Li, J.; Nelson, M. R.; Peng, C. Y.; Bashford, D.; Noodleman, L. *J. Phys. Chem. A* **1998**, *102*, 6311.
(2) Torres, R. A.; Lovell, T.; Noodleman, L.; Case, D. A. *J. Am. Chem. Soc.* **2003**, *125*, 1923.
(3) Sigfridsson, E.; Olsson, M. H. M.; Ryde, U. *Inorg. Chem.* **2001**, *40*, 2509.
(4) Sulpizi, M.; Raugei, S.; VandeVondele, J.; Carloni, P.; Sprik, M. *J. Phys. Chem. B* **2007**, *111*, 3969.
(5) Bashford, D.; Karplus, M.; Canters, G. W. *J. Mol. Biol.* **1988**, *203*, 507.
(6) Honig, B.; Nicholls, A. *Science* **1995**, *268*, 1144.
(7) Han, W. G.; Lovell, T.; Liu, T. Q.; Noodleman, L. *Inorg. Chem.* **2003**, *42*, 2751.
(8) Ullmann, G. M.; Noodleman, L.; Case, D. A. *J. Biol. Inorg. Chem.* **2002**, *7*, 632.
(9) Mao, J. J.; Hauser, K.; Gunner, M. R. *Biochemistry* **2003**, *42*, 9829.
(10) Warshel, A.; Papazyan, A.; Muegge, I. *J. Biol. Inorg. Chem.* **1997**, *2*, 143.
(11) Stephens, P. J.; Jollie, D. R.; Warshel, A. *Chem. Rev.* **1996**, *96*, 2491.
(12) Libeu, C. A. P.; Kukimoto, M.; Nishiyama, M.; Horinouchi, S.; Adman, E. T. *Biochemistry* **1997**, *36*, 13160.
(13) Ullmann, G. M.; Knapp, E. W. *Eur. Biophys. J. Biophys. Lett.* **1999**, *28*, 533.
(14) Popovic, D. M.; Zaric, S. D.; Rabenstein, B.; Knapp, E. W. *J. Am. Chem. Soc.* **2001**, *123*, 6040.
(15) Voigt, P.; Knapp, E. W. *J. Biol. Chem.* **2003**, *278*, 51993.
(16) Ishikita, H.; Knapp, E. W. *FEBS Lett.* **2005**, *579*, 3190.
(17) Botuyan, M. V.; ToyPalmer, A.; Chung, J.; Blake, R. C.; Beroza, P.; Case, D. A.; Dyson, H. J. *J. Mol. Biol.* **1996**, *263*, 752.

(18) Schutz, C. N.; Warshel, A. *Proteins: Struct., Funct., Genet.* **2001**, *44*, 400.
(19) Olsson, M. H. M.; Ryde, U. *J. Biol. Inorg. Chem.* **1999**, *4*, 654.
(20) Olsson, M. H. M.; Hong, G. Y.; Warshel, A. *J. Am. Chem. Soc.* **2003**, *125*, 5025.
(21) Li, H.; Webb, S. P.; Ivanic, J.; Jensen, J. H. *J. Am. Chem. Soc.* **2004**, *126*, 8010.
(22) Datta, S. N.; Sudhamsu, J.; Pandey, A. *J. Phys. Chem. B* **2004**, *108*, 8007.
(23) Sundararajan, M.; Hillier, I. H.; Burton, N. A. *J. Phys. Chem. A* **2006**, *110*, 785.
(24) Paraskevopoulos, K.; Sundararajan, M.; Surendran, R.; Hough, M. A.; Eady, R. R.; Hillier, I. H.; Hasnain, S. S. *Dalton Trans.* **2006**, 3067.
(25) Iozzi, M. F.; Cossi, M.; Improta, R.; Rega, N.; Barone, V. *J. Chem. Phys.* **2006**, *124*, 184103.
(26) Li, H.; Robertson, A. D.; Jensen, J. H. *Proteins: Struct., Funct., Bioinform.* **2004**, *55*, 689.
(27) Tapia, O.; Johannin, G. *J. Chem. Phys.* **1981**, *75*, 3624.
(28) Bonaccorsi, R.; Scrocco, E.; Tomasi, J. *Int. J. Quantum Chem.* **1986**, *29*, 717.
(29) Bonaccorsi, R.; Hodoscek, M.; Tomasi, J. *J. Mol. Struct.: Theochem* **1988**, *164*, 105.
(30) Bonaccorsi, R.; Ojalvo, E.; Tomasi, J. *Collect. Czech. Chem. Commun.* **1988**, *53*, 2320.
(31) Bonaccorsi, R.; Ojalvo, E.; Palla, P.; Tomasi, J. *Chem. Phys.* **1990**, *143*, 245.
(32) Bonaccorsi, R.; Floris, F.; Palla, P.; Tomasi, J. *Thermochim. Acta* **1990**, *162*, 213.
(33) Hoshi, H.; Sakurai, M.; Inoue, Y.; Chujo, R. *J. Chem. Phys.* **1987**, *87*, 1107.
(34) Cances, E.; Mennucci, B.; Tomasi, J. *J. Chem. Phys.* **1997**, *107*, 3032.
(35) Mennucci, B.; Cances, E.; Tomasi, J. *J. Phys. Chem. B* **1997**, *101*, 10506.
(36) Jorgensen, S.; Ratner, M. A.; Mikkelsen, K. V. *J. Chem. Phys.* **2001**, *115*, 3792.
(37) Jorgensen, S.; Ratner, M. A.; Mikkelsen, K. V. *Chem. Phys.* **2002**, *278*, 53.
(38) Jorgensen, S.; Ratner, M. A.; Mikkelsen, K. V. *J. Chem. Phys.* **2002**, *116*, 10902.
(39) Jorgensen, S.; Ratner, M. A.; Mikkelsen, K. V. *J. Chem. Phys.* **2001**, *115*, 8185.
(40) Sloth, M.; Jorgensen, S.; Bilde, M.; Mikkelsen, K. V. *J. Phys. Chem. A* **2003**, *107*, 8623.
(41) Im, W.; Feig, M.; Brooks, C. L. *Biophys. J.* **2003**, *85*, 2900.
(42) Tanizaki, S.; Feig, M. *J. Phys. Chem. B* **2006**, *110*, 548.
(43) Tanizaki, S.; Feig, M. *J. Chem. Phys.* **2005**, *122*, 124706.
(44) Feig, M.; Brooks, C. L. *Curr. Opin. Struct. Biol.* **2004**, *14*, 217.
(45) Moulinier, L.; Case, D. A.; Simonson, T. *Acta Crystallogr., Sect. D* **2003**, *59*, 2094.
(46) Si, D.; Li, H. *J. Chem. Phys.* **2009**, *131*, 044123.
(47) Hertwig, R. H.; Koch, W. *Chem. Phys. Lett.* **1997**, *268*, 345.
(48) Becke, A. D. *Phys. Rev. A* **1988**, *38*, 3098.
(49) Lee, C.; Yang, W.; Parr, R. G. *Phys. Rev. B* **1988**, *37*, 785.
(50) Schmidt, M. W.; Baldridge, K. K.; Boatz, J. A.; Elbert, S. T.; Gordon, M. S.; Jensen, J. H.; Koseki, S.; Matsunaga, N.; Nguyen, K. A.; Su, S. J.; Windus, T. L.; Dupuis, M.; Montgomery, J. A. *J. Comput. Chem.* **1993**, *14*, 1347.
(51) Gordon, M. S.; Schmidt, M. W. Advances in electronic structure theory: GAMESS a decade later. In *Theory and applications of computational chemistry*; Dykstra, C. E., Frenking, G., Kim, K. S., Scuseria, G. E., Eds.; Elsevier: Amsterdam, 2005.
(52) Berman, H. M.; Westbrook, J.; Feng, Z.; Gilliland, G.; Bhat, T. N.; Weissig, H.; Shindyalov, I. N.; Bourne, P. E. *Nucleic Acids Res.* **2000**, *28*, 235.
(53) Rodriguez, R.; Chinea, G.; Lopez, N.; Pons, T.; Vriend, G. *Bioinformatics* **1998**, *14*, 523.
(54) Roothaan, C. C. J. *Rev. Mod. Phys.* **1951**, *23*, 69.
(55) McWeeny, R.; Diercksen, G. *J. Chem. Phys.* **1968**, *49*, 4852.
(56) Francl, M. M.; Pietro, W. J.; Hehre, W. J.; Binkley, J. S.; Gordon, M. S.; Defrees, D. J.; Pople, J. A. *J. Chem. Phys.* **1982**, *77*, 3654.
(57) Rassolov, V. A.; Pople, J. A.; Ratner, M. A.; Windus, T. L. *J. Chem. Phys.* **1998**, *109*, 1223.
(58) Hart, P. J.; Nersissian, A. M.; Herrmann, R. G.; Nalbandyan, R. M.; Valentine, J. S.; Eisenberg, D. *Protein Sci.* **1996**, *5*, 2175.
(59) Kohzuma, T.; Inoue, T.; Yoshizaki, F.; Sasakawa, Y.; Onodera, K.; Nagatomo, S.; Kitagawa, T.; Uzawa, S.; Isobe, Y.; Sugimura, Y.; Gotowda, M.; Kai, Y. *J. Biol. Chem.* **1999**, *274*, 11817.
(60) Hall, J. F.; Kanbi, L. D.; Strange, R. W.; Hasnain, S. S. *Biochemistry* **1999**, *38*, 12675.
(61) Barrett, M. L.; Harvey, I.; Sundararajan, M.; Surendran, R.; Hall, J. F.; Ellis, M. J.; Hough, M. A.; Strange, R. W.; Hillier, I. H.; Hasnain, S. S. *Biochemistry* **2006**, *45*, 2927.
(62) Kanbi, L. D.; Antonyuk, S.; Hough, M. A.; Hall, J. F.; Dodd, F. E.; Hasnain, S. S. *J. Mol. Biol.* **2002**, *320*, 263.
(63) Barone, V.; Cossi, M. *J. Phys. Chem. A* **1998**, *102*, 1995.
(64) Li, H.; Jensen, J. H. *J. Comput. Chem.* **2004**, *25*, 1449.
(65) Su, P.; Li, H. *J. Chem. Phys.* **2009**, *130*, 074109.
(66) Rosen, D. *Trans. Faraday Soc.* **1963**, *59*, 2178.
(67) Bone, S.; Pethig, R. *J. Mol. Biol.* **1982**, *157*, 571.
(68) Bone, S.; Pethig, R. *J. Mol. Biol.* **1985**, *181*, 323.
(69) King, G.; Lee, F. S.; Warshel, A. *J. Chem. Phys.* **1991**, *95*, 4366.
(70) Antosiewicz, J.; McCammon, J. A.; Gilson, M. K. *J. Mol. Biol.* **1994**, *238*, 415.
(71) Li, H.; Robertson, A. D.; Jensen, J. H. *Proteins: Struct., Funct., Bioinform.* **2005**, *61*, 704.
(72) Jimenez, B.; Piccioli, M.; Moratal, J. M.; Donaire, A. *Biochemistry* **2003**, *42*, 10396.
(73) Krishnan, R.; Binkley, J. S.; Seeger, R.; Pople, J. A. *J. Chem. Phys.* **1980**, *72*, 650.
(74) Balabanov, N. B.; Peterson, K. A. *J. Chem. Phys.* **2005**, *123*, 064107.
(75) Hulsker, R.; Mery, A.; Thomassen, E. A.; Ranieri, A.; Sola, M.; Verbeet, M. P.; Kohzuma, T.; Ubbink, M. *J. Am. Chem. Soc.* **2007**, *129*, 4423.
(76) Ryde, U.; Olsson, M. H. M.; Pierloot, K.; Roos, B. O. *J. Mol. Biol.* **1996**, *261*, 586.
(77) Solomon, E. I.; Szilagyi, R. K.; George, S. D.; Basumallick, L. *Chem. Rev.* **2004**, *104*, 419.
(78) Ando, K. *J. Phys. Chem. B* **2004**, *108*, 3940.
(79) Ghosh, S.; Xie, X. J.; Dey, A.; Sun, Y.; Scholes, C. P.; Solomon, E. I. *Proc. Natl. Acad. Sci. U.S.A.* **2009**, *106*, 4969.
(80) Nersissian, A. M.; Immoos, C.; Hill, M. G.; Hart, P. J.; Williams, G.; Herrmann, R. G.; Valentine, J. S. *Protein Sci.* **1998**, *7*, 1915.
(81) Giudici-Orticoni, M. T.; Guerlesquin, F.; Bruschi, M.; Nitschke, W. *J. Biol. Chem.* **1999**, *274*, 30365.
(82) Hunt, A. H.; Toypalmer, A.; Assamunt, N.; Cavanagh, J.; Blake, R. C.; Dyson, H. J. *J. Mol. Biol.* **1994**, *244*, 370.
(83) McGinnis, J.; Ingledew, W. J.; Sykes, A. G. *Inorg. Chem.* **1986**, *25*, 3730.
(84) George, S. D.; Basumallick, L.; Szilagyi, R. K.; Randall, D. W.; Hill, M. G.; Nersissian, A. M.; Valentine, J. S.; Hedman, B.; Hodgson, K. O.; Solomon, E. I. *J. Am. Chem. Soc.* **2003**, *125*, 11314.
(85) Su, P. F.; Li, H. *J. Chem. Phys.* **2009**, *131*, 014102.
(86) Machczynski, M. C.; Gray, H. B.; Richards, J. H. *J. Inorg. Biochem.* **2002**, *88*, 375.
(87) Jensen, J. H.; Li, H. Calculation of Reduction Potential and pKa. In *Computational Inorganic and Bioinorganic Chemistry*; Solomon, E. I., Scott, R. A., King, R. B., Eds.; John Wiley & Sons, Ltd.: Chichester, UK, 2009.
(88) Malmstrom, B. G.; Leckner, J. *Curr. Opin. Chem. Biol.* **1998**, *2*, 286.
(89) Randall, D. W.; Gamelin, D. R.; LaCroix, L. B.; Solomon, E. I. *J. Biol. Inorg. Chem.* **2000**, *5*, 16.
(90) Gray, H. B.; Malmstrom, B. G.; Williams, R. J. P. *J. Biol. Inorg. Chem.* **2000**, *5*, 551.
(91) Guss, J. M.; Harrowell, P. R.; Murata, M.; Norris, V. A.; Freeman, H. C. *J. Mol. Biol.* **1986**, *192*, 361.
(92) Fields, B. A.; Bartsch, H. H.; Bartunik, H. D.; Cordes, F.; Guss, J. M.; Freeman, H. C. *Acta Crystallogr., Sect. D* **1994**, *50*, 709.
(93) Milani, M.; Andolfi, L.; Cannistraro, S.; Verbeet, M. P.; Bolognesi, M. *Acta Crystallogr., Sect. D* **2001**, *57*, 1735.
(94) Fields, B. A.; Duff, A. P.; Govinderaju, K.; Lee, M. P.; W., J. H.; Church, W. B.; Guss, J. M.; Sykes, A. G.; Freeman, H. C. Unpublished results.
(95) Armstrong, G. D.; Chapman, S. K.; Sisley, M. J.; Sykes, A. G.; Aitken, A.; Osheroff, N.; Margoliash, E. *Biochemistry* **1986**, *25*, 6947.
(96) Inoue, T.; Sugawara, H.; Hamanaka, S.; Tsukui, H.; Suzuki, E.; Kohzuma, T.; Kai, Y. *Biochemistry* **1999**, *38*, 6063.
(97) Romero, A.; De la Cerda, B.; Varela, P. F.; Navarro, J. A.; Hervas, M.; De la Rosa, M. A. *J. Mol. Biol.* **1998**, *275*, 327.
(98) Collyer, C. A.; Guss, J. M.; Sugimura, Y.; Yoshizaki, F.; Freeman, H. C. *J. Mol. Biol.* **1990**, *211*, 617.
(99) Redinbo, M. R.; Cascio, D.; Choukair, M. K.; Rice, D.; Merchant, S.; Yeates, T. O. *Biochemistry* **1993**, *32*, 10560.
(100) Xue, Y. F.; Okvist, M.; Hansson, O.; Young, S. *Protein Sci.* **1998**, *7*, 2099.
(101) Shibata, N.; Inoue, T.; Nagano, C.; Nishio, N.; Kohzuma, T.; Onodera, K.; Yoshizaki, F.; Sugimura, Y.; Kai, Y. *J. Biol. Chem.* **1999**, *274*, 4225.
(102) Sato, K.; Kohzuma, T.; Dennison, C. *J. Am. Chem. Soc.* **2003**, *125*, 2101.

JP905825Q